Fluidised glass façade elements for an active energy transmission control

D. Gstoehl[1], J. Stopper[2], S. Bertsch[3], D. Schwarz[1]

1 Universtiy of Liechtenstein, Vaduz, Liechtenstein
2 Technical University of Munich, Munich, Germany
3 Interstate University of Applied Sciences Buchs NTB, Buchs SG, Switzerland

Abstract: A fluidised glass façade element with two thermally separated fluid layers is proposed. This system replaces shading device, solar collector, cooling and heating element. The outer fluid layer acts as a control for the energy transmission by absorption of solar radiation, while the inner fluid layer regulates the inner surface temperature. The concept of the façade system is proven with a prototype. A basic heat transfer model is formulated resulting in stagnation temperatures of the outer fluid layer of up to 70°C at a solar irradiation of 1000 W/m^2. An average temperature of 40°C of the outer fluid results in a collector efficiency of approximately 50% for a solar irradiation of 600 W/m^2. The collector efficiency decreases strongly with decreasing solar radiation and increasing temperature of the collector. A correlation for the collector efficiency is given. It is expected that architects and engineers will receive a standardised product, which helps to increase the efficiency of their building significantly. The user-friendly plug and play system enables the use of renewable energy in an easy way throughout the whole façade. Because of the active control, the system can be used in every climate zone.

Keywords: solar energy, renewable engery, energy efficiency, building enveloppe

1. Introduction

A glass façade system which controls the energy flows within a transparent building envelope is proposed [1]. The façade enables perfect comfort in the building, while simultaneously reducing the energy demand. Two fluid filled layers are implemented in the glass façade. These two layers are regulating all energy flows within the facade. The inner fluid layer keeps the inside surface temperature just below or above room temperature for heating and cooling while the outer liquid layer controls the energy transmission by absorption of the solar irradiation [2]. The inside and outside fluid layers are thermally separated. Two basic operating modes for summer and winter are illustrated below.
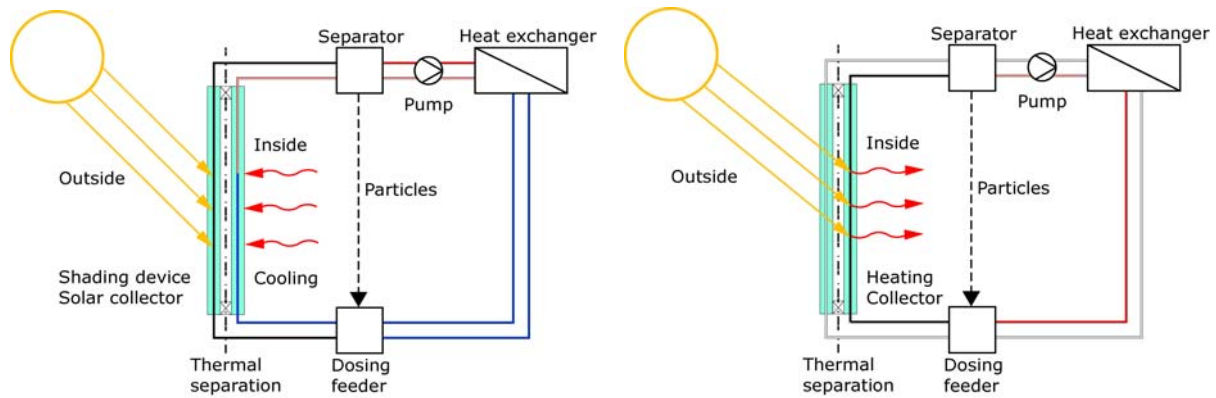
Daniel Gstoehl, daniel.gstoehl@uni.li

Figure 1 Basic operating modes in summer (left) and winter (right).

The absorption of solar irradiation within the fluid is controlled by addition and removal of particles. Both, the inner and outer liquid layer consist of separate circuits with particle feeder, particle separator, pump and heat exchanger. In the summer scenario particles are added to the outer layer for shading. In comparison to other shading devices the absorbed solar radiation is not lost. It can be transported by the fluid to another place to be used, e.g. backside of a building or a thermal storage such as the ground. While the outer facade is mostly darkened during summer, clear water is circulated inside the inner circuit. Its temperature is adjusted by the cooling system of the building in order to achieve a facade that can remove heat from the adjacent room. Due to a good thermal insulation between the outside and inside fluid layer, heat exchange between the two layers is small, reducing the cooling demand in summertime. During winter the outer liquid layer is clear or emptied. Therefore the solar radiation is absorbed inside the inner layer. Thus heat is obtained inside the insulated perimeter where it can be used for heating purposes. This system replaces the shading device, solar collector, cooling ceiling, floor heating, and insulating façade of a building within a thickness of a few centimetres. The transparent façade can help increase the energy efficiency of buildings in every climate zone and enables the use of renewable solar energy throughout the whole façade area.

2. Setup

For the proof of concept a prototype has been build. The prototype features two fluid layers separated by a thermal separation. A commercial triple-glazed insulation glass unit is used as thermal separation. It consists of three layers of 6 mm thick glass with gaps of 16 mm each. The gas is filled using the inert gas Krypton. Low-E coatings are on the inside surface of the outer pane and on the outside surface of the inner pane of the insulation glass unit. On both sides of the insulation glass unit, a 6 mm thick glass is placed to form the chambers for fluid 1 (outside) and fluid 2 (inside). The fluid chamber width is 2 mm, resulting in a total thickness of the glazing system of 66 mm. The complete glazing system is illustrated in Fig. 2. The clear glass is PLANILUX (zone 2, 6, 10) and the coated glass is PLANITHERM ONE II (zone 4 and 8), both from Saint-Gobain Glass.
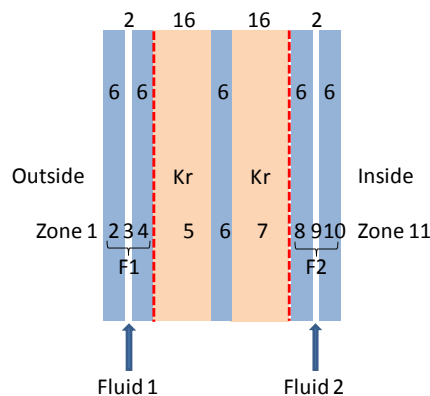

Figure 2 Glazing system consisting of two fluid chambers separated by an insulation glass unit.

The width and height of the prototype glazing system are 1 m and 1.6 m, respectively. The fluid enters both chambers at the bottom and leaves at the top of the façade element. Four inlets and four outlets are located on the glass of the interior and exterior side for each chamber. The fluid enters the chamber perpendicular to the flow direction as can be seen in the schematic in Fig. 3.

Figure 3 Left: Prototype façade element with 4 inlets at the bottom and 4 outlets at the top (1 m x 1.6 m). Right: Photograph of the upper part showing the positioning of the spacers by thin wires.

Downstream of the inlets, in the lower part of the façade element, a line of injection nozzles is placed in the fluid chamber. A second line of nozzles is placed in the upper part of the façade element. Inlet region and nozzles were designed to achieve a uniform flow distribution while keeping the pressure loss low along the width of the façade element. The geometry of the nozzles and results of an analysis using computational fluid dynamic (CFD) calculations are given in Fig. 4. Downstream of the nozzles the streamlines are equally distributed and straight indicating a homogenous flow field within the fluid chamber.
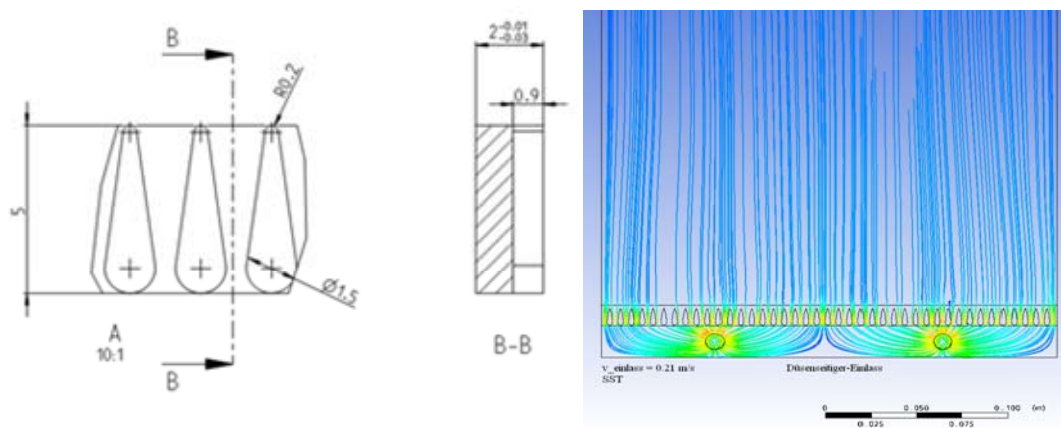

Figure 4 Left: Geometry of the nozzles. Right: Streamlines illustrating the uniform flow distribution.

The façade element is operated such that the pressure in the fluid chamber is always below the ambient pressure. This operation mode is chosen to minimize the glass thickness, since stress resulting from the pressure difference between water and surrounding air can be supported by small columns between the windows. The fluid is circulated by a pump located downstream of the façade element outlet and a fluid reservoir is located upstream of the façade element. This reservoir is positioned in a way that the free surface of the fluid is at the level of the inlet of the façade element. With this setup the static pressure of the fluid at the bottom of the façade element is close to ambient pressure. With increasing distance from the lower edge of the façade element the static pressure decreases in the fluid. At the top of the façade

element the static pressure is about 0.16 bar below ambient pressure. In order to assure a uniform distance between the glass layers forming the fluid chamber spacers are equally distributed as indicated in Fig. 3. The distance between the spacers is 100 mm and the diameter is 2 mm each. To keep the spacers in position, they are currently fixed on thin wires as shown in Fig. 3 on the right.

Preliminary tests were performed using a colorant (Basacid Black) to vary the absorptivity of the fluid. Two sequences of pictures of a duration of about 15 s are given in Fig. 5. Low shading and complete shading are illustrated in the top row and bottom row, respectively. At the beginning water is circulating in the façade element. In the following pictures the front of coloured water moves upwards. Thus, depending on the concentration of the colorant the transmission can be controlled continuously.
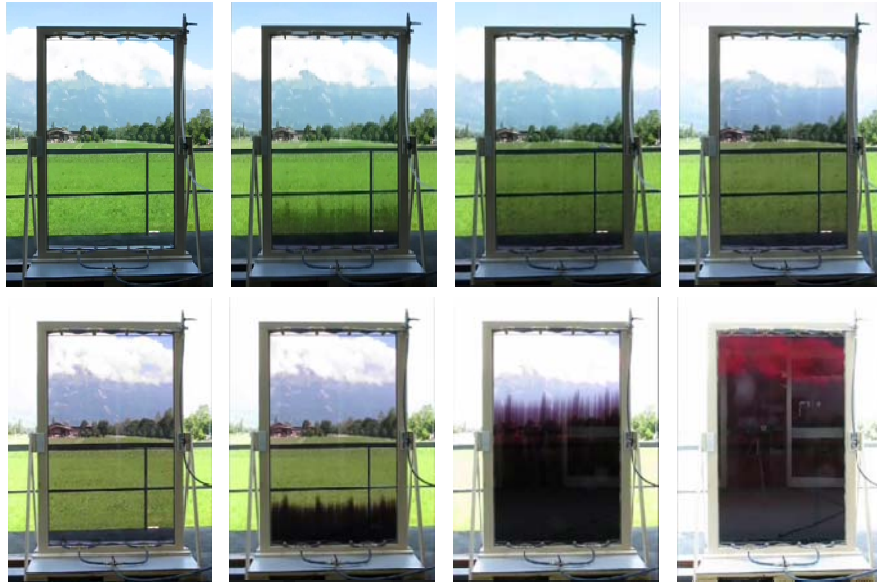

Figure 5 Preliminary tests using a colorant to vary the absorptivity. Top: low concentration of colorant. Bottom: high concentration of colorant. Note that the used camera automatically adjusted the brightness of the whole picture leading to an overexposure of image area around the façade element.

3. Modelling

A basic physical model of the façade system has been developed in order to determine the potential of the current setup. In a first step the absorbed solar radiation for all layers of the glazing system is determined. In the second step an energy balance is solved to obtain the resulting heat transfer rates and temperatures. The properties presented for the glazing system are calculated at normal incidence for the incoming angle.

Glass and liquid layer are considered as a semitransparent medium with properties averaged over the entire spectrum. The glazing system is divided into eleven zones as indicated in Fig. 2, zone 1 and zone 11 are outside and inside, respectively. The glass layers are zone 2, 4, 6, 8, and 10. The outer liquid layer is zone 3 and the inner liquid layer is zone 9. Reflection is considered at every interface between the zones. The reflectivity at normal incidence at interface between zone k and l, r_{kl}, is approximated by

$$r_{kl} = \left(\frac{n_k - n_l}{n_k + n_l} \right)^2$$

Where n_k and n_l are the refraction indices of the medium in zone k and zone l. The values of the refractive index used for the glass, fluid, and gas layer were $n_{glass}=1.5$, $n_{fluid}=1.33$ and $n_{gas}=1.0$. The low-E coating is modelled with an increased reflectivity of $r_{coating}=r_{45}=r_{78}=0.35$.

For every interface between zone k and l the following set of equations is formulated for the fraction of radiation, s, travelling in forward and backward direction

$$s_{kl.out.F} = (1 - r_{kl}) \cdot s_{kl.in.F} + r_{kl} \cdot s_{kl.in.B}$$

$$s_{kl.out.B} = (1 - r_{kl}) \cdot s_{kl.in.B} + r_{kl} \cdot s_{kl.in.F}$$

where the subscripts in / out stand for incoming / outgoing. F denotes for forward direction (outside to inside) and B for backward direction (inside to outside).

Absorption is taken into account only within the glass and liquid layers. The absorptivity of a single pass of the radiation through a glass layer was set to $a_{glass}=0.125$ according to the glass thickness. The absorptivity of the fluids is a parameter that was varied in the range of 0.1 to 0.9 in order to account for the change in absorptivity while shading. The fraction of the absorbed radiation (A) in forward and backward direction is expressed as

$$A_{Z1.F} = a_{Zl} \cdot s_{kl.out.F}$$

$$A_{Z1.B} = a_{Zl} \cdot s_{k+1l+1.out.B}$$

where a_{Zl} denotes the absorptivity of a single pass of the radiation through zone l. The total absorptivity of the zone l is the sum of both contributions in forward and backward direction, $A_{Zl}=A_{Zl.F}+ A_{Zl.B}$. Now the fraction of the incoming radiation at the next interface in forward direction can be calculated as

$$s_{k+1l+1.in.F} = s_{kl.out.F} - A_{Z1.F}$$

Correspondingly the fraction of incoming radiation at the next interface in backward direction is

$$s_{kl.in.B} = s_{k+1l+1.out.B} - A_{Z1.B}$$

These equations were formulated for all interfaces and the resulting system of equation was solved using EES from F-Chart Software. For a comparison a center-of-glazing modelling was performed with the software WINDOW 6.3 from the Lawrence Berkeley National Laboratory. For this reference calculation it was assumed that both liquid chambers were filled with air, since WINDOW cannot calculate fluid layers. Results are given in Table 1. The values obtained with the current model for the same condition are in excellent agreement for the transmissivity (T), reflectivity (R), and absorptivity (A) of the whole glazing system. To achieve this agreement $r_{coating}$ and a_{glass} were used as tuning parameters. The absorptivity of the individual zones, A_{Zn}, is in reasonable agreement, with a maximum deviation of less than 3% for the glass layer in the middle (zone 6).

Table 1 Reference calculations with air instead fluid. Transmissivity (T), reflectivity (R), and absorptivity (A) of the complete glazing system and the absorptivites for each individual zone (see Fig. 2).

	T	R	A	A_{Z2}	A_{Z3}	A_{Z4}	A_{Z6}	A_{Z8}	A_{Z9}	A_{Z10}
WINDOW 6.3	0.199	0.336	0.465	0.194	0	0.164	0.057	0.034	0	0.017
Current model	0.196	0.338	0.466	0.166	0	0.146	0.085	0.039	0	0.030

Based on the determined distribution of the absorbed radiation, heat transfer rates and fluid temperatures were determined in the next step. The convective heat transfer coefficient is set to 23 W/m²-K on the outside and 8 W/m²-K on the inside of the glazing system. The convective heat transfer coefficient within the fluid chamber is fixed at 440 W/m²-K⁻¹ [5]. Conduction is considered in the glass layers with $k_{glass}=0.76$ W/m-K. The thermal separation between both fluid chambers, zone 5 to 7, consisting of two gaps with gas fill and one glass layer is represented by a U-value of 0.5 W/m²-K.

For radiative heat transfer the glazing system is reduced to two opaque elements. Element F1 comprises zone 2, 3, and 4 and element F2 consists of zone 7, 8, and 9 as indicated in Fig. 2. Both elements have uniform temperature. The fluid and layer the adjacent glass layers are assumed to be at the same temperature. Radiative heat exchange is considered between outside and element F1, element F1 and element F2, and element F2 and the inside. The emissivity used for uncoated and the coated side of the glass were 0.837 and 0.013, respectively. The fraction of absorbed energy in zone 6, A_{Z6}, is attributed to both elements. The fraction of absorbed solar radiation in element F1 and F2 is $A_{F1}=A_{Z2}+A_{Z3}+A_{Z4}+A_{Z6}/2$ and $A_{F2}=A_{Z8}+A_{Z9}+A_{Z10}+A_{Z6}/2$.

4. Results

In order to determine the effect of the absorptivity of the fluid layers on the distribution of the solar irradiation within the glazing system a parametric study is performed. Results are summarized in Table 2. For the summer scenarios, the absorptivity of fluid 1 is varied between 0.9 and 1, while the absorptivity of fluid 2 is kept constant at 0.1 (clear water). For the winter scenarios, the absorptivity of fluid 1 is set to 0 (chamber emptied), while the absorptivity of fluid 2 is varied. In the summer up to 76% of the incoming radiation is absorbed by fluid 1, and in the winter up to 21% is absorbed by fluid 2.

Table 2 Parametric study for the absorptivity of the fluid layers. Transmissivity (T), reflectivity (R), and absorptivity (A) of the complete glazing system and the absorptivites for each individual zone (see Fig. 2).

	a_{fluid1}	a_{fluid2}	T	R	A	A_{Z2}	A_{Z3}	A_{Z4}	A_{Z6}	A_{Z8}	A_{Z9}	A_{Z10}
Summer	0.9	0.1	0.018	0.071	0.911	0.125	0.755	0.014	0.008	0.004	0.002	0.003
	0.7	0.1	0.054	0.091	0.855	0.128	0.632	0.044	0.025	0.011	0.007	0.008
	0.5	0.1	0.090	0.131	0.779	0.134	0.485	0.073	0.042	0.019	0.012	0.014
	0.3	0.1	0.127	0.193	0.680	0.144	0.311	0.103	0.059	0.026	0.017	0.020
	0.1	0.1	0.165	0.276	0.560	0.156	0.111	0.133	0.077	0.034	0.023	0.025
Winter	0.0	0.9	0.020	0.334	0.646	0.165	0.000	0.145	0.084	0.036	0.213	0.003
	0.0	0.7	0.059	0.334	0.607	0.165	0.000	0.145	0.084	0.036	0.167	0.009
	0.0	0.5	0.099	0.334	0.567	0.165	0.000	0.145	0.084	0.037	0.120	0.015
	0.0	0.3	0.139	0.335	0.526	0.165	0.000	0.145	0.084	0.037	0.073	0.021
	0.0	0.1	0.180	0.335	0.485	0.166	0.000	0.145	0.084	0.037	0.025	0.028

The stagnation temperature and the collector efficiency for the outer liquid layer were determined. Results for the summer case for different absorptivities of the outer fluid layer are given in Table 3. The incoming solar radiation is set to $q_{sol}=600$ W/m^2. The absorbed solar energy is $q_{sol.F1}=A_{F1}\cdot q_{sol}$ in element F1 and $q_{sol.F2}=A_{F2}\cdot q_{sol}$ in element F2. The outside and inside temperatures are set to 30°C and 20°C, respectively. In all calculations the temperature of the inner fluid layer, T_{F2}, is also kept constant at 20°C. To achieve this, the heat flux, q_{F2} has, to be removed by fluid 2. In the first set of calculations, no heat is removed by fluid 1 ($q_{F1}=0$). The resulting temperature of fluid 1 is thus its stagnation temperature. For the absorption of roughly 540 W/m^2 a stagnation temperature of 54°C is reached. Most of the absorbed energy in element 1, $q_{F1toZ1}=520$ W/m^2, is transferred to the outside, while only a small fraction of 3% passes the thermal separation. With decreasing absorptivity of fluid 1 the stagnation temperature decreases due to a smaller fraction of the energy being absorbed in fluid 1. This also results in a higher absorption in fluid 2 and an increased cooling demand for fluid 2. In the second set of calculations the average temperature of fluid 1 is fixed at 40°C. The heat transfer to the outside, inside, and between the layers is therefore constant. For absorptivity of fluid 1, $a_{fluid1}=0.9$, a heat flux of 310 W/m^2 is achieved within the outer element at an average temperature of 40°C. This corresponds to a collector efficiency of $\eta=q_{F1}/q_{sol}=51\%$. The energy collected by fluid 1 decreases with decreasing absorptivity of fluid 1.

Stagnation temperatures of fluid 1 as a function of absorptivity of fluid 1 for different incoming solar radiation are illustrated in Fig. 6. Stagnation temperatures up to 70°C are reached for an incoming solar radiation of 1000 W/m^2. This is below the boiling point of water at the top of the façade element that is at 90°C due to the reduced pressure.

Collector efficiencies for different values of solar radiation and average temperatures of fluid 1 are shown in Fig 7. The collector efficiency decreases strongly with decreasing solar radiation and increasing temperature of the collector.

Table 3 Heat transfer rates and resulting temperatures for different summer scenarios. Incoming solar radiation is set to q_{sol}=600W/m^2.

|	a_{fluid1} -	a_{fluid2} -	$q_{sol.F1}$ W/m^2	$q_{sol.F2}$ W/m^2	q_{F1toZ1} W/m^2	q_{F1toF2} W/m^2	q_{F1} W/m^2	q_{F2} W/m^2	T_{F1} °C	T_{F2} °C	η %
Stagnation	0.9	0.1	538.8	7.8	520.6	18.2	0	26.0	53.7	20	0
	0.7	0.1	489.6	23.4	472.6	17.0	0	40.4	51.5	20	0
	0.5	0.1	427.8	39.6	412.3	15.5	0	55.1	48.8	20	0
	0.3	0.1	352.2	55.8	338.5	13.7	0	69.5	45.5	20	0
	0.1	0.1	263.4	72.6	251.8	11.6	0	84.2	41.5	20	0
Fixed Temp.	0.9	0.1	538.8	7.8	218.2	10.7	309.8	18.5	40	20	51.6
	0.7	0.1	489.6	23.4	218.2	10.7	260.6	34.1	40	20	43.4
	0.5	0.1	427.8	39.6	218.2	10.7	198.8	50.3	40	20	33.1
	0.3	0.1	352.2	55.8	218.2	10.7	123.2	66.5	40	20	20.5
	0.1	0.1	263.4	72.6	218.2	10.7	34.44	83.3	40	20	5.7
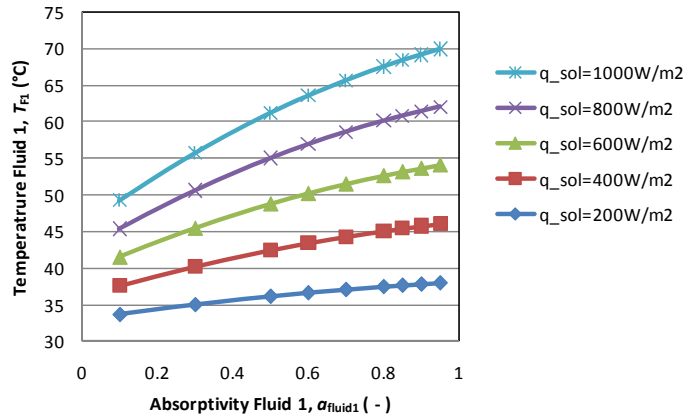
Figure 6 Stagnation temperatures for different values of solar radiation (summer scenario).

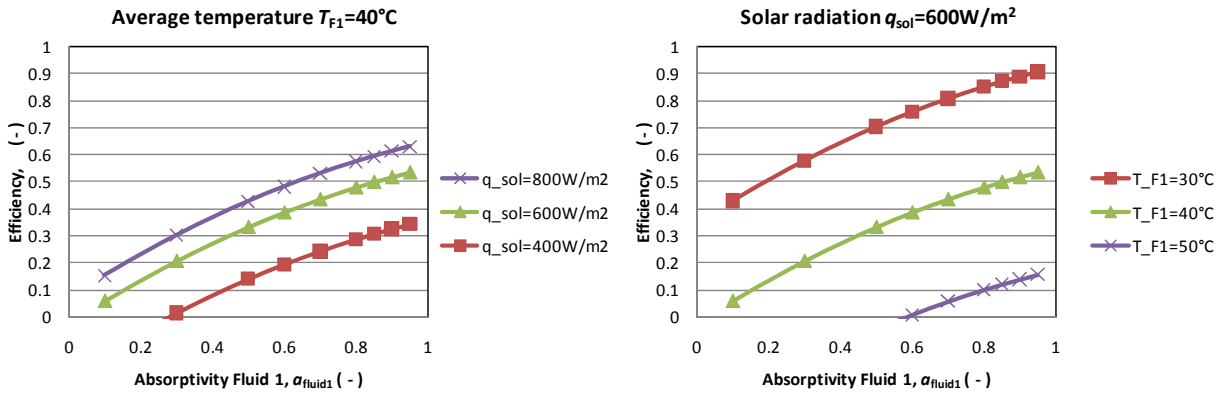**Figure 7** Left: collector efficiency for different values of solar radiation (T_{F1}=40°C). Right: collector efficiency for different collector temperatures (q_{sol}=600W/m^2).

For the summer case presented above ($a_{\text{fluid2}}=0.1$), the collector efficiency can be correlated with:

$$\eta = \eta_0 - c_1 \frac{T_{F1} - T_1}{q_{sol}} - c_2 \frac{\left(T_{F1} - T_1\right)^2}{q_{sol}}$$

Where η_0 is the maximum efficiency that depends on the absorptivity of the fluid: $\eta_0 = 0.3475 + 0.8473 \cdot a_{\text{fluid1}} - 0.2733 \cdot a_{\text{fluid1}}^2$. The first and second order loss coefficient were found to be $c_1 = 26.04$ W/m^2-K and $c_2 = -0.3679$ W/m^2-K^2 within the ranges of $T_{F1} = 30$ to 50°C and $q_{sol} = 400$ to 800 W/m^2. The correlation above is within a relative deviation to the numerical model of smaller than 1%.

5. Summary and Conclusion

A fluidised glass façade element with two fluid layers is proposed that unifies the functions of a shading device, solar collector, cooling and heating element. The concept of the façade system could be proven with a prototype. The challenges of handling the static pressure, uniform distribution of the liquid within the layers and sealing issues could be successfully addressed. For the simulation of the thermal behaviour a basic heat transfer model has been formulated resulting in stagnation temperatures of the outer fluid layer in the range of 45°C to 70°C at an incoming solar radiation ranging from 400 to 1000 W/m2. For an average fluid temperature of 40°C, the collector efficiency is estimated to be approximately 50% at an incoming solar radiation of 600 W/m^2. In a next step the current model will be expanded to allow for different angles of the incoming radiation. A two band approach (the complete solar and the visible spectrum) will be pursued to additionally investigate transmission and reflection of the light. After validation of the simulation buildings equipped with the new façade system will be simulated in order to determine their performance in different climate zones. It is expected that architects and engineers will receive a standardised product, which increases the efficiency of their building significantly. The user-friendly plug and play system enables the use of renewable energy in an easy way. Because of the active control, the system can be used in every climate zone and for every building type.

References

[1] Patent WO 98/51973.

[2] Patent Switzerland, Registration no. 02163/10

[3]   Wymann, J.-P., 2004, Wasserdurchströmtes Glas, Tec21, 29-30, pp. 14-17. (www.tec21.ch/archiv/)

[4] Hube, W., Platzer, W., and Schwarz, D., 2004, Entwicklung eines flüssigkeitdurchströmten Fassadensystems zur Solarenergiekontrolle und -nutzung, 14. Symposium Thermische Solarenergie, Staffelstein.

[5] Incropera, F.P., DeWitt, D.P., 2002, Fundamentals of Heat and Mass Transfer, 5th Edition, Wiley.

Acknowledgements